Society For Biomaterials

Influence of membrane cholesterol and substrate elasticity on endothelial cell spreading behavior

Zhongkui Hong,[1,2] Ilker Ersoy,[3] Mingzhai Sun,[4] Filiz Bunyak,[3] Paul Hampel,[1] Zhenling Hong,[1] Zhe Sun,[2] Zhaohui Li,[2] Irena Levitan,[5] Gerald A. Meininger,[2] Kannappan Palaniappan[3]

[1]Department of Physics and Astronomy, University of Missouri, Columbia, Missouri 65211
[2]Dalton Cardiovascular Research Center, and Department of Pharmacology and Physiology, University of Missouri, Columbia, Missouri 65211
[3]Department of Computer Science, University of Missouri, Columbia, Missouri 65211
[4]Davis Heart and Lung Research Institute, The Ohio State University, Ohio 43210
[5]Pulmonary, Critical Care & Sleep Medicine, College of Medicine, University of Illinois-Chicago, Chicago, Illinois 60612

Received 27 June 2012; revised 15 October 2012; accepted 24 October 2012
Published online in Wiley Online Library (wileyonlinelibrary.com). DOI: 10.1002/jbm.a.34504

Abstract: Interactions between implanted materials and the surrounding host cells critically affect the fate of bioengineered materials. In this study, the biomechanical response of bovine aortic endothelial cells (BAECs) with different membrane cholesterol levels to polyacrylamide (PA) gels was investigated by measuring cell adhesion and spreading behaviors at varying PA elasticity. The elasticity of gel substrates was manipulated by cross-linker content. Type I collagen (COL1) was coated on PA gel to provide a biologically functional environment for cell spreading. Precise quantitative characterization of changes in cell area and perimeter of cells across two treatments and three bioengineered substrates were determined using a customized software developed for computational image analysis. We found that the initial response of endothelial cells to changes in substrate elasticity was determined by membrane cholesterol levels, and that the extent of endothelial cell spreading increases with membrane cholesterol content. All of the BAECs with different cholesterol levels showed little growth on substrates with elasticity below 20 kPa, but increased spreading at higher substrate elasticity. Cholesterol-depleted cells were consistently smaller than control and cholesterol-enriched cells regardless of substrate elasticity. These observations indicate that membrane cholesterol plays an important role in cell spreading on soft biomimetic materials constructed with appropriate elasticity. J Biomed Mater Res Part A: 00A: 000–000, 2012.

Key Words: cell spreading, cell image segmentation, membrane cholesterol, vascular grafts, polyacrylamide gel

How to cite this article: Hong Z, Ersoy I, Sun M, Bunyak F, Hampel P, Hong Z, Sun Z, Li Z, Levitan I, Meininger GA, Palaniappan K. 2012. Influence of membrane cholesterol and substrate elasticity on endothelial cell spreading behavior. J Biomed Mater Res Part A 2012:00A:000–000.

INTRODUCTION

Autologous vessel grafting is often the primary choice in the treatment of late-stage cardiovascular diseases.[1] However, some patients do not have suitable tissue for harvest because of extensive damage; in such cases, synthetic vascular implants are becoming more prevalent compared with heterogeneous allografts. Biocompatible synthetic materials and tissue engineering are beginning to offer a variety of clinically viable alternatives to vessel transplantation.[2] Flexible and bridgeable polymers are a promising biocompatible material that is grafted to replace damaged blood vessels.[3,4] However, a number of issues need to be addressed in using synthetic biomaterials, including the response and integration of host endothelial cells to the grafted synthetic materials.[5] In addition to the vascular grafting, the synthetic materials have also attracted a broad attention in tissue engineering. However, the success rate of implantation surgery depends critically on the vascularization of the newly formed tissue to receive nutrients, expel metabolites, and integrate with the surrounding host tissue.[6–8]

Better understanding of the interaction between vascular endothelial cells and the surrounding extracellular material is necessary for the successful clinical application of synthetic vascular grafts and to promote angiogenesis in engineered tissues. Furthermore, atherosclerotic patients typically have high cholesterol levels in blood and tissue cells. Therefore, it is of specific interest for vascular tissue engineering to investigate the response of host endothelial cells with varying cholesterol levels to an engineered material.

Vascular endothelial cells are anchorage dependent, and without attachment to a substrate, they will eventually die.[9] The properties of the substrate markedly influence cellular functions and properties such as cell adhesion, spreading,

Correspondence to: Z. Hong; e-mail: kuihong@gmail.com
Contract grant sponsor: U.S. National Institute of Health awards; contract grant numbers: R33 EB00573, HL083298, 1P01HL095486

migration, signaling, and mechanotransduction through substrate ligand–receptor interactions.[10,11] Moreover, the cellular and biomechanical functions of endothelial cells are directly involved in their response to the surrounding tissue and cells, and this could potentially regulate the angiogenesis in implanted biomedical materials. Cholesterol is an important component of the animal cell membrane. Multiple studies have shown that membrane cholesterol affects endothelial biomechanics by changing the integrity of the cell membrane or regulating the interaction between the plasma membrane and underlying cytoskeleton.[12–14] In a previous study, it was also reported that cholesterol depletion of endothelial cells significantly decreases cell deformation in response to mechanical force.[15,16]

In this article, we investigate the attachment and spreading behavior of bovine aortic endothelial cells (BAECs) with different membrane cholesterol levels on polyacrylamide (PA) gel substrates. The results show that cholesterol plays a critical role in the temporal response of BAECs to the change of substrate elasticity. Cholesterol-depleted cells have much higher elongation values than cholesterol-enriched and control cells for different elasticity of substrates. Cholesterol enrichment stimulates cell membrane protrusions and accelerates cell spreading in comparison with cholesterol-depleted and control cells.

MATERIALS AND METHODS

Deactivation and activation of glass coverslips

Glass coverslips were deactivated before covering with PA gel preparations. To deactivate, the glass coverslips (18 × 18 mm) were washed with ethanol and distilled water. After drying, 50 μL dimethyldichlorosilane (SUPELCO, Bellefonte, PA) was uniformly layered on the coverslip surface and air dried. The deactivated coverslips were used for covering the PA gel (see below). In a separate process, a second set of glass coverslips (18 × 18 mm) were activated for PA gel attachment. A 100 μL solution of sodium hydroxide (0.1*N*; Fisher Scientific, Pittsburgh, PA) was smeared onto glass coverslips (18 × 18 mm) that were pretreated by passing through the inner flame of a gas burner. After air drying for 10–20 min, a sodium hydroxide thin film was formed on the surface of the coverslips. Then, 100 μL 3-aminopropyltrimethoxysilane was homogenously covered onto the sodium hydroxide layer. After air drying for 10–20 min, the coverslips were rinsed with flowing deionized water to thoroughly wash away the free 3-aminopropyltrimethoxysilane (Sigma Aldrich, St. Louis, MO). The coverslips were then submerged in 0.5% glutaraldehyde (Fluka) in phosphate-buffered saline solution for 30 min. The coverslips were subsequently rinsed multiple times with distilled water on a shaker and air dried overnight.

Preparation of PA gel substrates with varying elasticity

The soft substrates for cell spreading assessment were prepared by polymerization of PA on the chemically modified glass coverslips as described below.[11] PA gels composed of 10 (w/v)% acrylamide solution were prepared by dissolution of 1 g acrylamide powder (Sigma Aldrich) into 10 mL of deionized water. A total of 0.005–0.035 g *N*,*N*'-methylene bisacrylamide powder (Sigma Aldrich), 50 μL ammonium

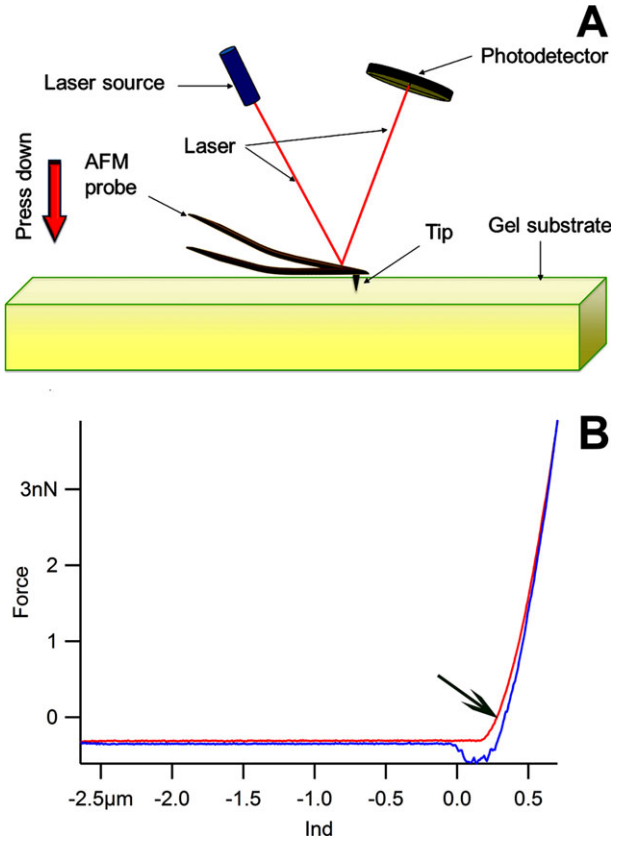

FIGURE 1. Diagrammatic scheme showing elasticity measurement on PA gel substrate using AFM (A). Force curves recorded by AFM (B). Arrow indicates the indentation part of force curve (red = approaching curve) beginning at point of curve inflection. [Color figure can be viewed in the online issue, which is available at wileyonlinelibrary.com.]

persulfate (10%) (Sigma Aldrich) solution, and 5 μL *N*,*N*,*N*',*N*'-tetramethylethylenediamine (Sigma Aldrich) were added subsequently to the acrylamide solution. A 25-μL portion of the reaction mixture was rapidly pipetted onto the activated coverslip and carefully covered with a deactivated coverslip. After the solution reacted for 30 min at room temperature, the upper coverslips were carefully removed and the gel was gently rinsed three times for 10 min with HEPES (50 m*M*) on a shaker.

Coating PA gels with type I collagen (COL1)

N-Sulfosuccinimidyl-6-[4′-azido-2′-nitrophenylamino] hexanoate (Sulfo-SANPAH; PIERCE, Rockford, IL) was used to cross-link COL1 molecules onto the surface of the PA gel. A total of 200 μL of sulfo-SANPAH (1 m*M*) was carefully pipetted onto the drained PA gel surface, and the surface was exposed to UV light for 10 min. The gel was gently washed twice for 10 min with HEPES (50 m*M*) at a pH of 8.5 on a shaker. After the last HEPES solution was aspirated, 200 μL COL1 (0.3 mg/mL) (Type I Rat tail; Sigma, St. Louis, MO) was covered on the top of PA gel, and then incubated at 4°C overnight.

Characterization of substrate elasticity and topography

An atomic force microscope (AFM, model: MFP-3D BIO™; Asylum Research, Santa Barbara, CA) mounted on an

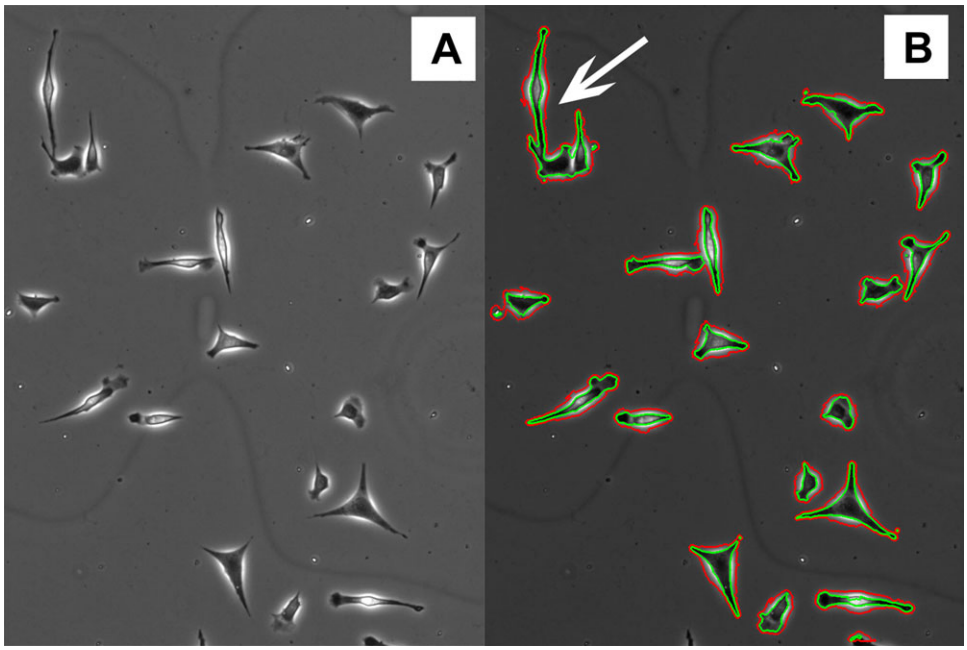

FIGURE 2. A sample raw image of cholesterol-depleted cell on gel substrate (A). The result of automatic cell boundary detection by our algorithm (B). The arrow indicates clustered cells. To avoid the effect that cell-to-cell contact could have on cell spreading behaviour, only the healthy single cells were selected to compute the cell area and cell shape. Red contours were initial detections by using the ridge detection. Green contours were the refined cell boundaries by our level set active contour algorithm. The length of green contour was computed as the perimeter of each cell and interior area of green contour was computed as cell area. [Color figure can be viewed in the online issue, which is available at wileyonlinelibrary.com.]

Olympus IX81 microscope (Olympus) with a silicon nitride cantilever (model: MLCT; Bruker, Santa Barbara, CA) was used to measure the Young's modulus of elasticity of PA gel substrates (Fig. 1). Each cantilever used in the experiments was calibrated using thermal noise amplitude analysis before a given measurement.[17,18] The measurement was performed in accordance with the principle described in the literature.[19–21] In brief, the pyramidal tip AFM probe was used to repeatedly indent and retract from the substrate surface at 0.5 Hz (tip speed 4 μm/s) to collect 50 force curves from the same site on each substrate. For each experiment, three different sites were randomly selected from the midway between the center and margin of substrate to collect a total of 150 force curves per substrate with Asylum MFP-3D software (Asylum Research). The Hertz model was used to obtain the following expression between the force (F) loaded on the surface of the substrate by the cantilever and the corresponding indentation depth (δ) of a soft gel:

$$F = \frac{2}{\pi} \times \tan(\alpha) \times \frac{E}{1-\upsilon^2} \times \delta^2 \qquad (1)$$

where E is Young's modulus, ν is the Poisson ratio of the substrate, and α is half the opening angle of the indenting cone. Because the PA gel networks can be accurately modeled as having the elasticity properties of rubber, a Poisson ratio $\nu = 0.5$ and half opening angle $\alpha = 18.75^\circ$ was used.[19] The Asylum MFP-3D BIO^{TM} AFM and the Bruker MLCT silicon nitride cantilever were also used to obtain topographical surface images of the PA gel substrate. AFM was operated in contact mode, and the AFM probe was scanned across 20 × 20 μm of the substrate surface at 0.2 Hz of scan rate with a tracking force of approx. 500 pN. The height and deflection image data were acquired using the Asylum MFP-3D Software.

Cell culture, cholesterol depletion, and enrichment

BAECs between passages 10 and 15 were cultured in Dulbecco's modified eagle's medium (DMEM; Cell Grow, Washington, DC) supplemented with 10% fetal bovine

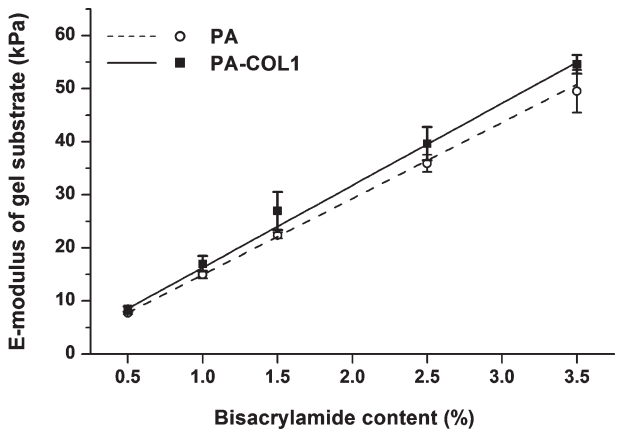

FIGURE 3. The plot of *E*-modulus of substrate against the content of cross-linker within the PA gel. Content of cross-linker indicates the mass percentage of bisacrylamide to acrylamide in PA gel. The *E*-modulus of multilayer substrates was determined by fitting a Hertz model to the 100–200 nm of the indentation curve recorded by AFM. There was no effect of Col1 coating on PA gel stiffness. Error bars represent standard deviation obtained from the experimental data points.

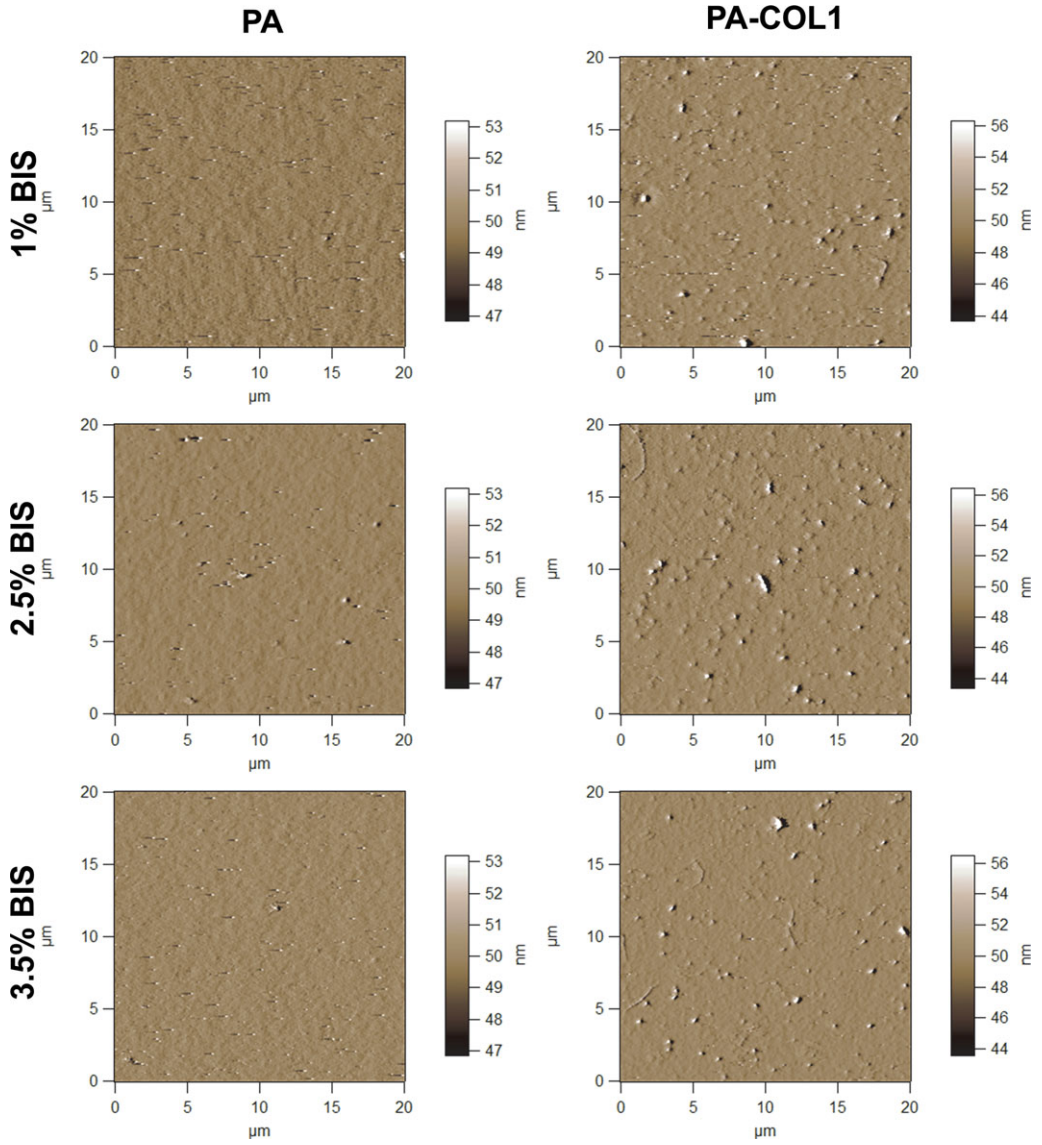

FIGURE 4. The topography of gel substrate acquired by AFM at different bisacrylamide content relative to acrylamide. Bisacrylamide content in PA gel did not affect the COL1 coating characteristics of the gel and had no significant impact on the topography of the final gel substrates. [Color figure can be viewed in the online issue, which is available at wileyonlinelibrary.com.]

serum (FBS; Atlanta Biologicals, Lawrenceville, GA). Cell cultures were maintained in a humidified incubator at 37°C with 5% CO_2. The cells were fed and passed every 2–3 days. BAECs with different membrane cholesterol levels were used in this study: cholesterol-depleted, cholesterol-enriched, and normal BAECs as control. Membrane cholesterol was depleted by incubation in 5 m*M* methyl-β-cyclodextrin (MβCD; Sigma, St. Louis, MO) in serum-free medium for 1 h. For membrane cholesterol enrichment, BAECs were exposed to methyl-β-cyclodextrin (5 m*M*) saturated with cholesterol (Sigma Aldrich) in serum-free medium for 1 h.[15]

Phase-contrast microscopy for cell morphology measurements

BAECs at different cholesterol levels were seeded onto substrates with varying rigidities and incubated in serum-free medium at 37°C with 5% CO_2. Stain-free live cell imaging of endothelial cells on gel substrates using noninvasive phase-contrast microscopy was used to record the visual appearance changes in BAEC shape over time. The BAEC imaging was performed at several time intervals. All imagery was captured at room temperature in serum-free medium using an OLYMPUS IX-70 microscope mounted with a Photometrics CoolSNAP CCD imager using a 20× objective lens. The viewing region covered a spatial extent of 877 by 695 μm with spatial sampling resolution of 0.675 μm in x and y directions and resulted in digital images that were 1300 × 1030 pixels in size, which were saved in TIFF format using Image-Pro capture software. Images were acquired at specific time intervals of 2, 6, and 24 h in each experiment to measure the progress of cell spreading behavior, and typically, 10 images were captured per experiment (combination of substrate

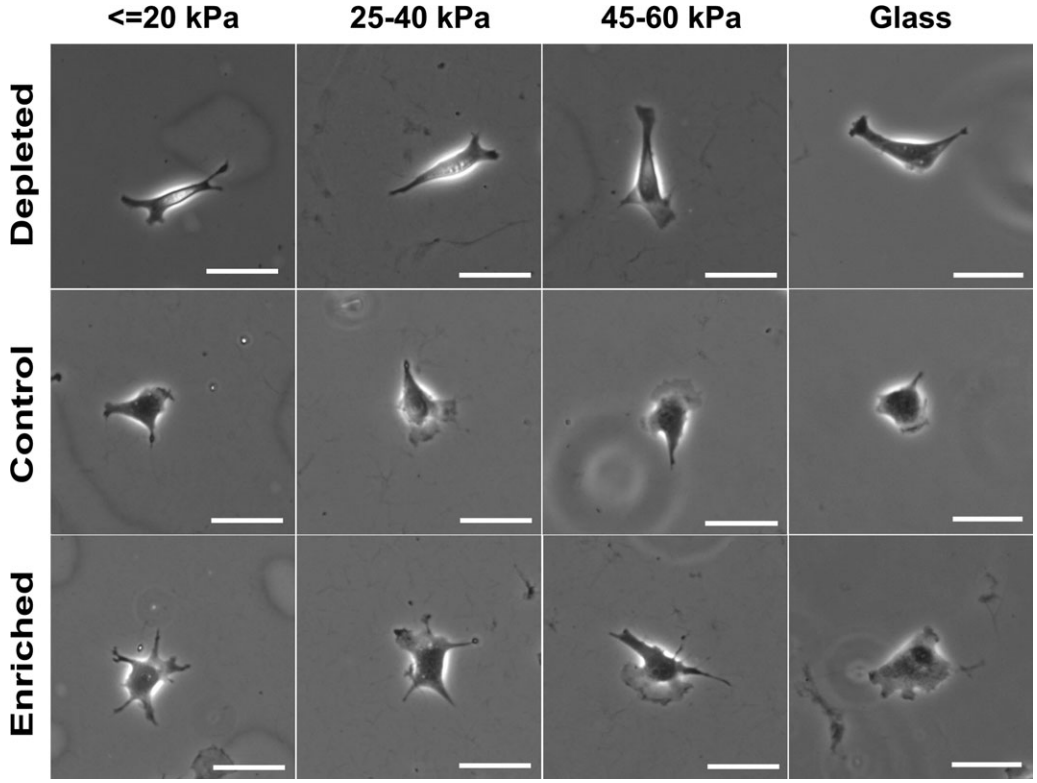

FIGURE 5. Representative images of cell spreading behavior for the BAECs with different membrane cholesterol levels after culturing for 2 h are shown for three different gel substrates elasticity and glass. Scale bars are 50 μm.

elasticity, cell membrane cholesterol level and time); five gels for a given modulus (i.e., substrate elasticity) were tested with two to three images per gel. Each image typically included 15–20 cells within the microscope field of view.

Quantitative measurement of cell area and perimeter

Digital cytometry was used to analyze images for cell morphology. We developed automatic cell segmentation software for objective and reproducible image-based quantitative measurement of cell area, perimeter, and elliptical axes.[22] The geodesic active contour (GAC) model[23,24] of boundary representation and adaptation and level set methods have become increasingly popular for the automatic detection of cell boundaries.[25] For statistically reliable measures of cell spreading, accurate cell boundary segmentation, and area measurement, we developed the edge profile-guided active contour (EPAC) algorithm,[22,23] which makes fewer segmentation errors and obtains segmentations close to true cell boundaries (Fig. 2). A two-stage method of automatic initialization and contour evolution was used where cells were automatically detected in the first step using principal curvature-based ridgeness [red contours in Fig. 2(B)]. This initial approximate segmentation is used as the starting cell boundary that is refined using a level set-based curve evolution implementation of our novel edge profile-guided active contour method.[22,23] The EPAC algorithm evolves the initial segmentation more accurately, closer to the true cell boundaries and was validated by quantitatively comparing the automatic segmentation results with manually drawn cell boundaries by several domain experts. EPAC produces an average area measurement error of just 2.3%, whereas the classical GAC underestimates the cell area by an average of 28.6% because of excessive leakage. Details of the level set active contour formulation and quantitative evaluation were described in previous publications.[22,23] The EPAC method detects accurate cell boundaries from which reliable area and perimeter measurements for each of the isolated nontouching cells were estimated.

Cell-to-cell contact has a significant effect on cell spreading behavior that affects the statistical properties of single cell measurements. Therefore, only single cells were selected to analyze the changes in cell area and cell shape in a supervised manner. Data for the clustered cells, as indicated by arrow in Figure 2(B), were omitted in the current analysis to exclude the confounding influence of cell-to-cell contact. Cell area is computed for each image based on the pixel measurements of automatically segmented cell images and plotted against incubation time. In addition, to further characterize the differences in cell spreading behavior between BAECs with different cholesterol levels, we also computed the ratio of cell area to perimeter (APR) that has units of length. The inverse of APR was referred to as the shape factor[10] and used to characterize the relative number of extensions per unit length to differentiate between isotropic (i.e., circular shape) and anisotropic (i.e., polarized shape) cell spreading and adhesion. The APR continually increases with isotropic growth as the area increases faster than the perimeter by a factor proportional to the cell

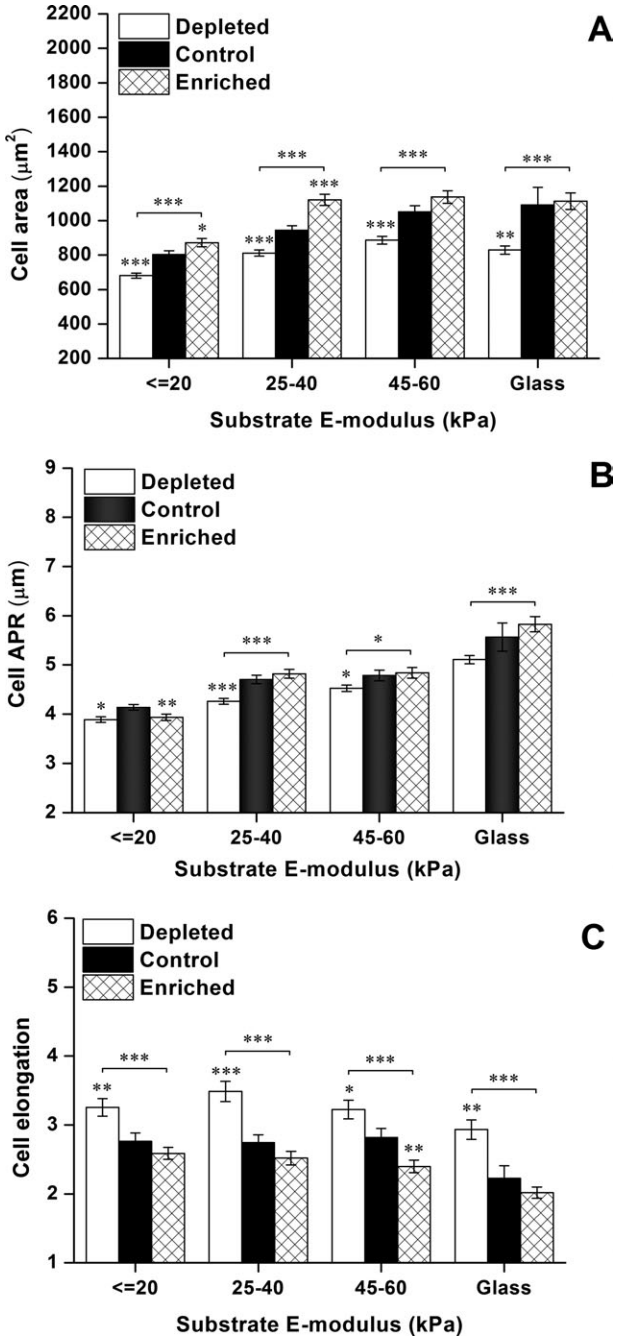

FIGURE 6. Variation in cell area (A), APR (B), and cell elongation (C) versus substrate elasticity for BAECs with different membrane cholesterol levels cultured for 2 h. About 100–200 cells were analyzed for each data point. Data are Mean ± SEM. $*p < 0.05$, $**p < 0.01$, $***p < 0.001$ (Tukey's test). Asterisks above bars represent the significance level of each population compared with respective control.

radius. Low values of the APR, approaching a limit of one, are indicative of spindle-like growth or many lamellipodia protrusions. Similarly, we computed cell elongation as the ratio of major axis length to minor axis length, measured from the shapes of segmented cells. To statistically characterize the difference in cell area and shape parameters between the BAECs with different cholesterol levels, the EPAC software was used to measure the properties of approximately 100–200 cells for each data point in plots described in the experimental results section.

Statistical analysis

Substrate elasticity data were expressed as the mean and standard deviation. Two sample *t* test was used to compare the elasticity of substrate before and after COL1 coating. A *p* value of <0.05 was considered as significant difference between two groups. Cell spreading data were expressed using mean and standard error of mean (SEM). A one-way analysis of variance (ANOVA) with Tukey's test was used to compare the cell spreading data of cholesterol-enriched, cholesterol-depleted, and control on the same substrate at the statistical significance level of $*p < 0.05$, $**p < 0.01$, *and* $***p < 0.001$. A two-way ANOVA was used to statistically analyze the effect of cholesterol level and substrate elasticity on the cell spreading behavior at the statistical significance level of $*p < 0.05$, $**p < 0.01$, *and* $***p < 0.001$.

RESULTS

Effect of COL1 grafting on the elasticity and topography of PA gel substrates

Cell attachment and polarization was studied by preparing a series of soft-gel substrates with varying rigidity by polymerization of 10% acrylamide in water solution containing bisacrylamide. Bisacrylamide was used as the cross-linker in the PA gel network to adjust the rigidity of multilayer gel substrates. Figure 3 shows that elasticity of the gel substrate has a linear response from 7 to 60 kPa as bisacrylamide concentration increases from 0.5 to 3.5% relative to acrylamide. Grafting of COL1 on PA gel did not significantly change the substrate elasticity ($p > 0.05$). Figure 4 shows the topography of PA gel before and after COL1 coating. PA gel substrates without COL1 coating exhibited a relatively flat topography with little spherical particles scattered on the surface (left panels of Fig. 4). After COL1 coating on the top of PA gel, substrates showed a fibrous deposition texture with some COL1 cluster scattered on the surface (right panels of Fig. 4). In addition, the PA gel topography (left panels of Fig. 4) does not change by increasing the bisacrylamide content. The variation in the composition of PA gel has no significant effect on the COL1 grafting behavior and no effect on the final gel substrate topography.

Cell attachment and shape on PA gels of varying substrate elasticity

Figure 5 shows BAECs with different membrane cholesterol levels attached to PA gel substrates with three different rigidity values and glass after 2 h. On the softest substrate, all BAECs with different membrane cholesterol levels respond to the substrate and attach to it. The cholesterol-depleted cells show a relatively compact and elongated cell shape in comparison with the relatively well spread profile of cholesterol-enriched and control cells. With increasing substrate rigidity, the cell area and cell shape of BAECs with different membrane cholesterol levels develop distinctive morphologies. Average cell area [Fig. 6(A)], APR [Fig. 6(B)], and cell elongation [Fig. 6(C)] of BAECs with different membrane cholesterol levels were computed and plotted against the substrate

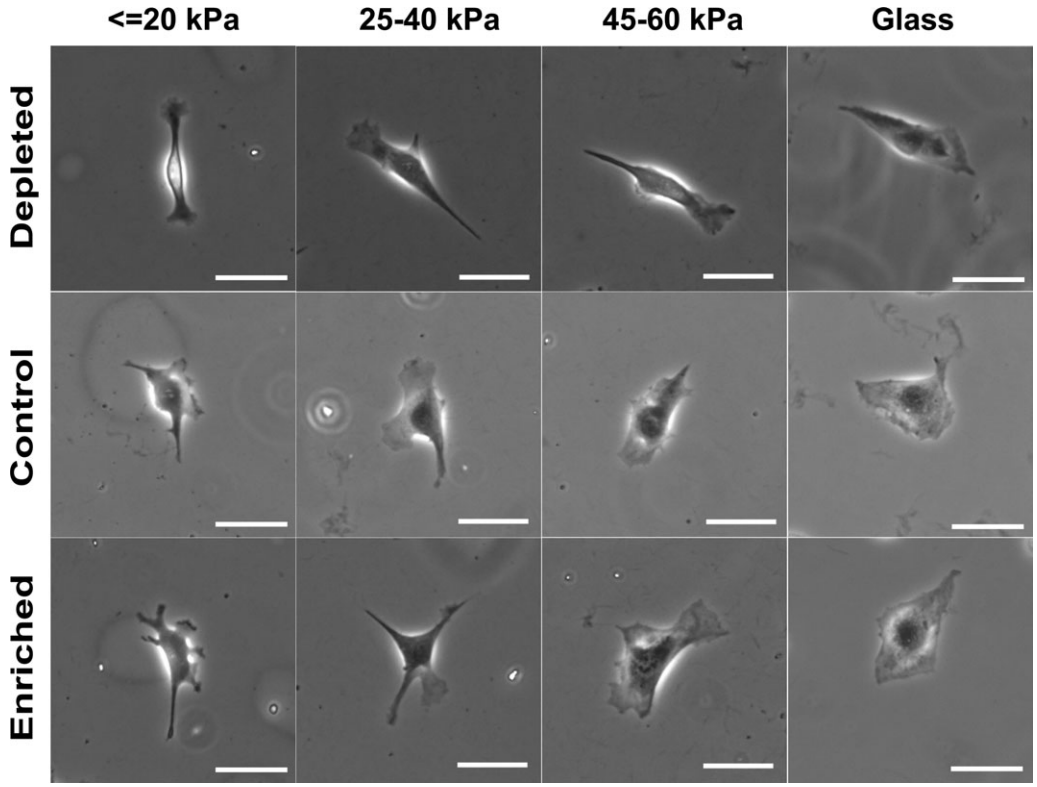

FIGURE 7. Representative cell spreading behavior after 6 h for the BAECs with different membrane cholesterol levels on gel and glass under different initial membrane cholesterol levels. Scale bars are 50 μm.

elasticity. After 2 h of incubation, the cell area of cholesterol-enriched and control cells is higher than that of cholesterol-depleted cells consistently across gels of at varying rigidity and glass. APR also shows a similar result as cell area; the cholesterol-enriched cells and control cells exhibit a higher APR than cholesterol-depleted cells. However, the cell elongation data show an opposite trend. Cholesterol-depleted cells have much higher elongation values than cholesterol-enriched and control cells for different elasticity, including glass.

Changes in cell area and cell shape with the incubation time

Figure 7 shows the representative morphology of BAECs with different membrane cholesterol levels cultured for 6 h on gel substrates and glass. The quantitative analysis of cell area, APR, and elongation of BAECs at different cholesterol levels is shown in Figure 8. The plots show the cholesterol-specific dependency of cell shape on substrate elasticity. On the soft substrate, a significant difference in spreading behavior was observed for BAECs with different membrane cholesterol levels. Cholesterol-depleted cells keep the compact and elongated cell shape at the early stages of cell spreading (Figs. 5 and 7), whereas the control and cholesterol-enriched cells show more spiky edges that characterizes spreading morphology with many more lamellipodia protrusions (Figs. 5 and 7). Specifically, the APR of cholesterol-enriched cells is close to that of control and cholesterol-depleted cells; on glass it is slightly lower than that of control cells [Fig. 8(B)], despite its higher cell area among the BAECs with different membrane cholesterol levels at 6 h of incubation [Fig. 8(A)]. The cell elongation of cholesterol-depleted cells is significantly higher than that of control and cholesterol-enriched cells [Fig. 8(C)].

As shown in Figure 9, after 24 h of culture, all of the BAECs with different membrane cholesterol levels show a smoother cell contour, i.e., less membrane protrusion than at the earlier stage of cell spreading (Fig. 5), except for the extremely soft PA substrate ($\leq$20 kPa). The summarized data [Fig. 10(A)] show that the area of the control cells is almost equal to the cholesterol-enriched cells, but the cholesterol-depleted cells have smaller area than the control and cholesterol-enriched cells. The change in cell APR is shown in Figure 10(B). The APR of cholesterol-enriched cells is similar to that of the control cells but larger than that of the cholesterol-depleted cells. It reflects a change in the shape of cells to a less spiky and smooth contour after 24 h of incubation. Cholesterol-depleted cells still show a more elongated cell shape compared with control and cholesterol-enriched cells except those cultured on the extremely soft substrate ($\leq$20 kPa). In summary, all BAECs with different membrane cholesterol levels show a similar tendency of variation in cell area as the change in substrate elasticity, that is, small area on soft gel and becoming well spread with increasing substrate elasticity. However, cholesterol depletion delays cell spreading. Over a 24-h observation period, the cholesterol-depleted cells show an elongated cell shape, whereas the cholesterol-enriched cells exhibit a much spikier cell shape than control and

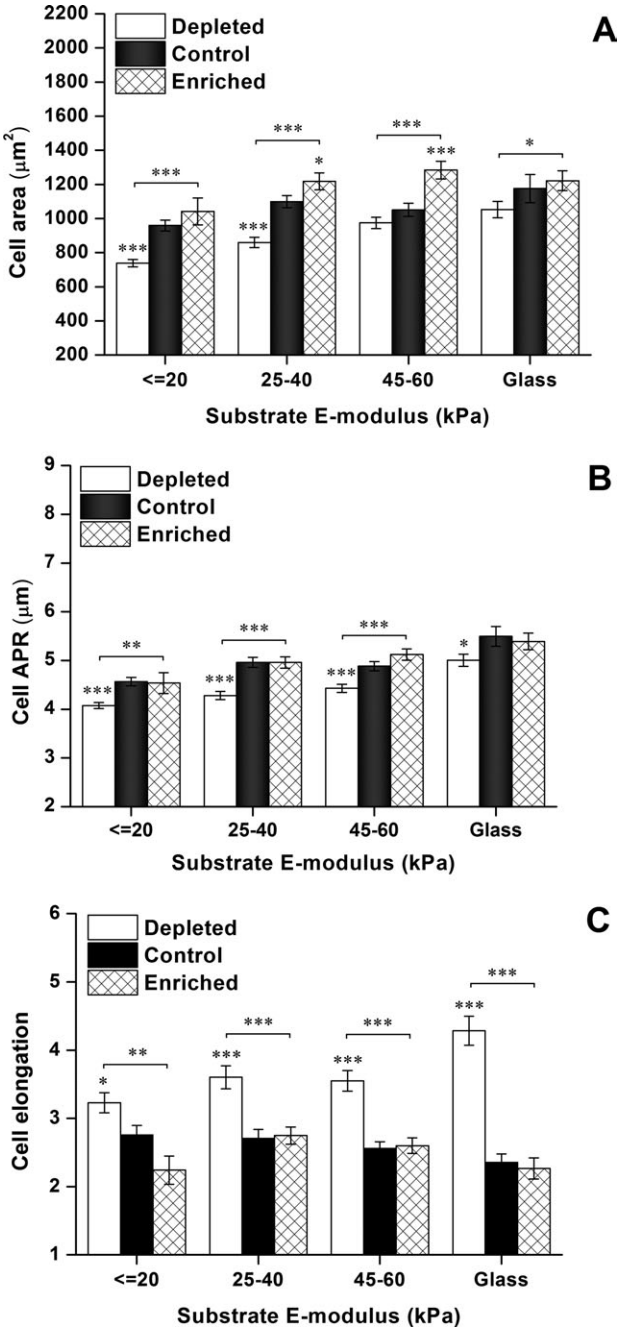

FIGURE 8. Cell area (A), APR (B), and cell elongation (C) of BAECs with different membrane cholesterol levels cultured for 6 h on gel substrate and glass. The data points of A, B, and C represent the average value of 100–200 cells. Data are Mean ± SEM. $*p < 0.05$, $**p < 0.01$, $***p < 0.001$ (Tukey's test). Asterisks above bars represent the significance level of each population compared with respective control.

cholesterol-depleted cells. The result of a two-way ANOVA is listed in Table I. The effect of variation in cholesterol level and substrate elasticity significantly influences cell spreading for each individual treatment and all times. However, the interaction of the two factors has a more significant influence on cell elongation than on cell area or cell APR for longer periods of incubation.

Effect of gel elasticity and membrane cholesterol level on cell viability

As shown in Figure 9, after 24 h of incubation on soft substrate, the cholesterol-enriched and cholesterol-depleted cells almost round up on soft substrates, whereas the control cells maintain their spread morphology. From the cell area data [Fig. 10(A)] on the soft PA gel substrate (≤20 kPa), we can see a decrease in cell area for cholesterol-enriched cells in comparison with the earlier stage of the incubation [Fig. 8(A)]. It is also noted from elongation data [Fig. 10(C)] that after 24 h of incubation, the elongation of cholesterol-depleted cells cultured on a soft substrate (≤20 kPa) decreases to almost the same as control and cholesterol-enriched cells, whereas on stiffer substrates, cholesterol-depleted cells remain elongated. These data indicate that the viability of cholesterol-enriched and cholesterol-depleted cells on soft substrate was lower than control cells.

DISCUSSION

Lu et al.[26] reported that the more quickly an engineered surface becomes covered with an endothelial layer, the less likely are issues to arise that lead to restenosis and thrombosis. In addition, the vascularization of tissue-engineered devices also determine their success rate in medical applications.[27] Recent reports suggested that physical properties of hydrogel biomaterials, such as surface topography and compliance, significantly affect gene expression,[28] cell orientation, elongation, proliferation, and migration of vascular endothelial cells.[29–31] All of these endothelial behaviors are important for the remodeling of matrix, ingrowth of new vessels during wound healing, and for the interaction of native endothelial cells with implanted scaffolds. Recent publications have also reported that dysregulation of the endothelium would result in the modification of the extracellular matrix (ECM) and thickness and pliability of the vascular basement membrane.[4,32–36]

In this study, PA gel was selected as soft substrate for its high transparency and ease of controlling the elasticity by changing of bisacrylamide content. Because of the lack of the ligand for the cell attachment and spreading,[37] a thin film of COL1 gel was grafted on top of the PA gel by the covalent linkage of photoactive cross linker, sulfo-SANPAH, to provide a biologically functional environment. Changing bisacrylamide content in this study does not significantly affect the PA gel topography and COL1 coating behavior. Therefore, our studies were mainly focused on the impact of cellular cholesterol on endothelial cell behaviors at varying substrate elasticity levels rather than the effect of the texture of substrate. Our results clearly demonstrated the differential response of vascular endothelial cells to the change of PA gel elasticity. In this work, the most interesting finding was that the cholesterol-enriched cells were easier to attach on soft PA gel substrate and triggered the cell spreading rapidly in comparison with cholesterol-depleted cells and control. Another interesting finding of this research was that cholesterol-depleted cells showed the compact and elongated cell shape, whereas the control and

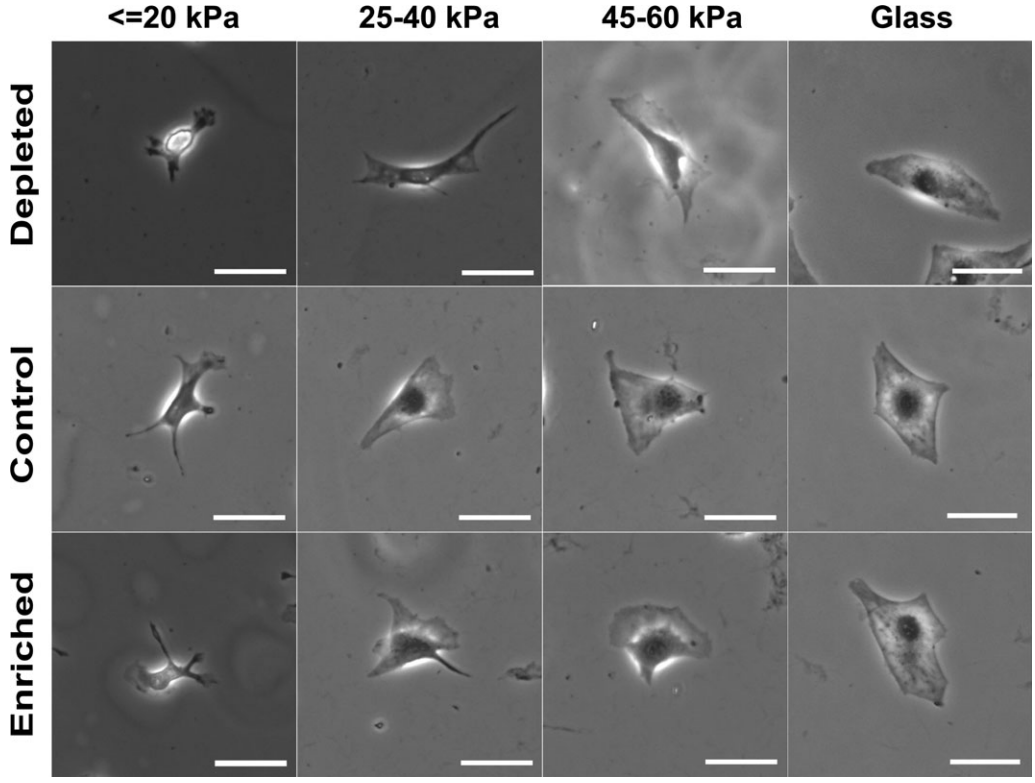

FIGURE 9. The representative cell images of BAECs at different cholesterol level spread for 24 h on glass and gel substrate with varying elasticity. Scale bars are 50 μm.

cholesterol-enriched cells exhibited a more isotropic spreading morphology with many more lamellipodia protrusions. It has been reported that the elongated endothelial cells exhibited a lower inflammation, decreased intercellular adhesion molecule expression, and were less atherogenic, leading to the success of prosthetics and the maintenance of homeostasis in the endothelial layer that was newly covered on a denuded region of vessel.[38,39]

What is the possible mechanism underlying cholesterol-dependent mechanosensitivity of endothelial cells? Cell spreading involves a series of cellular processes, for example, cell attachment, protrusion of lamellipodia, membrane ruffling, and cytoskeleton remodeling. It is known that integrin and cytoskeleton are involved in all of these cell motility processes. Signal transduction from extracellular matrix (ECM) to cytoplasm is achieved through the complex of integrin and cytoskeleton. The aim of this study was to elucidate how the membrane cholesterol regulates the response of endothelial cells to extracellular stimulation. To answer this question, we should clarify the relationship between membrane cholesterol and integrin adhesion, cytoskeleton, and their combination. In a recent study, we observed that cholesterol depletion could induce endothelial cells to become stiffer.[15] Cholesterol can regulate the polymerization of actin filaments and the organization of stress fibers through the lipid rafts and caveolae-mediated pathways.[40,41] Both lipid rafts and caveolae are cholesterol-dependent microdomains that can facilitate the interaction between transmembrane proteins and cytoskeleton. On the basis of these reports, we can interpret our results as follows: cholesterol enrichment increases the number of caveolae and lipid rafts on the cell membrane and stimulates the formation of new cytoskeleton, consequently driving the membrane protrusion and cell spreading. On the contrary, cholesterol depletion decreases the number of lipid rafts[42] and caveolae, which dissociates the integrin and cytoskeleton complex and blocks signal transduction between ECM and cytoplasm. In addition, cholesterol depletion increases membrane tension[12] and leads to the inhibition of lamellipodia protrusion and cell spreading.[43]

Cell shape and cell spreading is strongly regulated by intrinsic cellular processes and structure. However, the extracellular mechanical stimuli also influence cell biomechanics via signal transduction through the complex pathway involving the ECM–integrin–cytoskeletal axis and numerous actin-related proteins. Engler et al.[37] have found that increasing substrate rigidity induced the formation of stress fibers, which are necessary for cell spreading and cell movement. Yeung et al.[11] also reported that integrin expression increased with the elevation of substrate elasticity, and that cell spreading behavior was regulated by changing substrate elasticity. In our experiments, we also found significant differences in cell shape and spreading behavior of endothelial cells on substrates with different rigidity. The movement and spreading of animal cells on solid tissue or substrate is achieved by protrusion of membrane and cytoskeleton remodeling.[44] In this regard, the rigidity of a substrate, on which the cells are anchored and spread, should

be high enough to provide a counterforce to endure the contraction force of a cell for spreading and movement.

CONCLUSIONS

The results of our experiments showed that changing the bisacrylamide content in PA gels did not affect the COL1 coating characteristics of the gel and had no significant impact on the topography of the final gel substrates. The biomimetically designed soft substrates markedly impact endothelial cell attachment and spreading. The basic elasticity of PA hydrogel substrate that can support cell attachment and successful spreading was 25–60 kPa. Membrane cholesterol regulated the mechanosensitivity and fluidity of endothelial cells and subsequently affected the response of endothelial cells to extracellular stimulation. Cholesterol enrichment stimulated lamellipodia protrusion on soft gel and rapidly triggered cell spreading and isotropic growth, whereas membrane cholesterol depletion delayed cell spreading on soft substrate and led to more elongated cell morphology. These observations suggested that changing membrane cholesterol in combination with controlling the compliance of a synthetic hydrogel or other scaffold biomaterial could be critical factors in improving the biophysiochemical environment for transplanted materials in tissue engineering applications.

TABLE I. Two-way ANOVA Results for Three BAECs Morphology Parameters

	Cell Area (2, 6, and 24 h)	Cell APR (2, 6, and 24 h)	Cell Elongation (2, 6, and 24 h)
Cholesterol level	***, ***, ***	***, ***, ***	***, ***, ***
Substrate elasticity	***, ***, ***	***, ***, ***	***, —, **
Interaction	***, —, —	**, —, —	—,***, ***

—: $p > 0.05$, *: $p < 0.05$, **: $p < 0.01$, ***: $p < 0.001$.

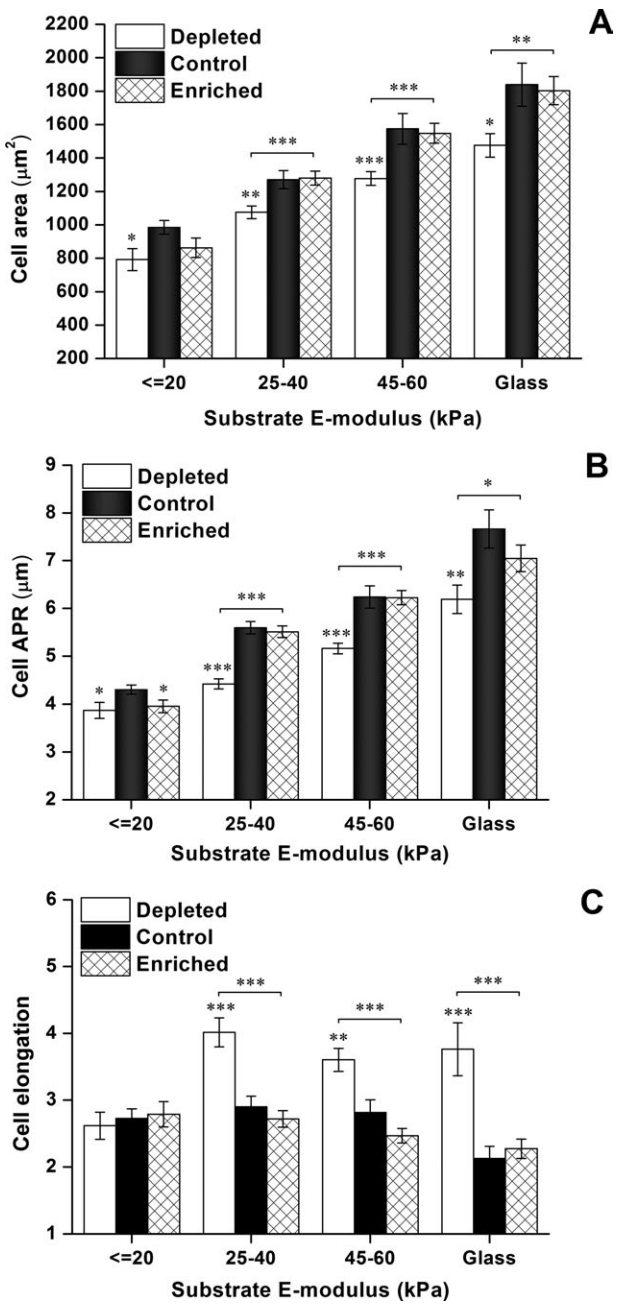

FIGURE 10. Cell area (A), APR (B), and cell elongation (C) of BAECs with different membrane cholesterol levels after 24 h on gel substrate with different elasticity. About 100–200 cells were analyzed for each data point. *$p < 0.05$, **$p < 0.01$, ***$p < 0.001$ (Tukey's test). Asterisks above bars represent the significance level of each population compared with respective control.

ACKNOWLEDGMENTS

The authors acknowledge Dr. Gabor Forgacs for the insightful discussions and support of the research.

REFERENCES

1. Campbell GR, Campbell JH. Development of tissue engineered vascular grafts. Curr Pharm Biotechnol 2007;8:43–50.
2. Langer R, Vacanti JP. Tissue engineering. Science 1993;260: 920–926.
3. Zustiak SP, Leach JB. Hydrolytically degradable poly(ethylene glycol) hydrogel scaffolds with tunable degradation and mechanical properties. Biomacromolecules 2010;11:1348–1357.
4. Wood JA, Liliensiek SJ, Russell P, Nealey PF, Murphy CJ. Biophysical cueing and vascular endothelial cell behavior. Materials 2010;3:1620–1639.
5. Wood JA, Shah NM, McKee CT, Hughbanks ML, Liliensiek SJ, Russell P, Murphy CJ. The role of substratum compliance of hydrogels on vascular endothelial cell behavior. Biomaterials 2011;32:5056–5064.
6. Leu A, Stieger SM, Dayton P, Ferrara KW, Leach JK. Angiogenic response to bioactive glass promotes bone healing in an irradiated calvarial defect. Tissue Eng Part A 2009;15:877–885.
7. Jain RK. Molecular regulation of vessel maturation. Nat Med 2003;9:685–693.
8. Carano RA, Filvaroff EH. Angiogenesis and bone repair. Drug Discov Today 2003;8:980–989.
9. Discher DE, Janmey P, Wang YL. Tissue cells feel and respond to the stiffness of their substrate. Science 2005;310:1139–1143.
10. Reinhart-King CA, Dembo M, Hammer DA. The dynamics and mechanics of endothelial cell spreading. Biophys J 2005;89: 676–689.
11. Yeung T, Georges PC, Flanagan LA, Marg B, Ortiz M, Funaki M, Zahir N, Ming W, Weaver V, Janmey PA. Effects of substrate stiffness on cell morphology, cytoskeletal structure, and adhesion. Cell Motil Cytoskeleton 2005;60:24–34.

12. Kwik J, Boyle S, Fooksman D, Margolis L, Sheetz MP, Edidin M. Membrane cholesterol, lateral mobility, and the phosphatidylinositol 4,5-bisphosphate-dependent organization of cell actin. Proc Natl Acad Sci USA 2003;100:13964–13969.
13. Levitan I, Shentu TP. Impact of oxLDL on cholesterol-rich membrane rafts. J Lipids 2011;2011:730209.
14. Kowalsky GB, Byfield FJ, Levitan I. oxLDL facilitates flow-induced realignment of aortic endothelial cells. Am J Physiol Cell Physiol 2008;295:C332–C340.
15. Sun M, Northup N, Marga F, Huber T, Byfield FJ, Levitan I, Forgacs G. The effect of cellular cholesterol on membrane-cytoskeleton adhesion. J Cell Sci 2007;120(Pt 13):2223–2231.
16. Byfield FJ, Tikku S, Rothblat GH, Gooch KJ, Levitan I. OxLDL increases endothelial stiffness, force generation, and network formation. J Lipid Res 2006;47:715–723.
17. Butt HJ, Jaschke M. Calculation of thermal noise in atomic force microscopy. Nanotechnology 1995;6:1–7.
18. Hutter JL, Bechhoefer J. Calibration of atomic-force microscope tips. Rev Sci Instrum 1993;64:1868–1873.
19. Domke J, Radmacher M. Measuring the elastic properties of thin polymer films with the atomic force microscope. Langmuir 1998; 14:3320–3325.
20. Rotsch C, Jacobson K, Radmacher M. Dimensional and mechanical dynamics of active and stable edges in motile fibroblasts investigated by using atomic force microscopy. Proc Natl Acad Sci USA 1999;96:921–926.
21. Lin DC, Dimitriadis EK, Horkay F. Robust strategies for automated AFM force curve analysis. I. Non-adhesive indentation of soft, inhomogeneous materials. J Biomech Eng 2007;129:430–440.
22. Ersoy I, Bunyak F, Palaniappan K, Sun M, Forgacs G. Cell spreading analysis with directed edge profile-guided level set active contours. Lect Notes Comput Sci (MICCAI)2008;5241(Pt 1):376–383.
23. Ersoy I, Bunyak F, Mackey MA, Palaniappan K. Cell segmentation using Hessian-based detection and contour evolution with directional derivatives. 15th IEEE Int. Conf. on Image Processing; San Diego, CA, USA: 2008. p 1804–1807.
24. Yezzi A Jr, Kichenassamy S, Kumar A, Olver P, Tannenbaum A. A geometric snake model for segmentation of medical imagery. IEEE Trans Med Imaging 1997;16:199–209.
25. Hafiane A, Bunyak F, Palaniappan K. Fuzzy clustering and active contours for histopathology image segmentation and nuclei detection. Lect Notes Comput Sci (ACIVS) 2008;5259:903–914.
26. Lu J, Rao MP, MacDonald NC, Khang D, Webster TJ. Improved endothelial cell adhesion and proliferation on patterned titanium surfaces with rationally designed, micrometer to nanometer features. Acta Biomater 2008;4:192–201.
27. Kannan RY, Salacinski HJ, Sales K, Butler P, Seifalian AM. The roles of tissue engineering and vascularisation in the development of micro-vascular networks: A review. Biomaterials 2005;26: 1857–1875.
28. Gasiorowski JZ, Liliensiek SJ, Russell P, Stephan DA, Nealey PF, Murphy CJ. Alterations in gene expression of human vascular endothelial cells associated with nanotopographic cues. Biomaterials 2010;31:8882–8888.
29. Liliensiek SJ, Wood JA, Yong J, Auerbach R, Nealey PF, Murphy CJ. Modulation of human vascular endothelial cell behaviors by nanotopographic cues. Biomaterials 2010;31:5418–5426.
30. McGuigan AP, Sefton MV. The influence of biomaterials on endothelial cell thrombogenicity. Biomaterials 2007;28:2547–2571.
31. Brandl F, Sommer F, Goepferich A. Rational design of hydrogels for tissue engineering: Impact of physical factors on cell behavior. Biomaterials 2007;28:134–146.
32. Engler AJ, Griffin MA, Sen S, Bonnemann CG, Sweeney HL, Discher DE. Myotubes differentiate optimally on substrates with tissue-like stiffness: Pathological implications for soft or stiff microenvironments. J Cell Biol 2004;166:877–887.
33. Gama Sosa MA, Gasperi RD, Rocher AB, Wang AC, Janssen WG, Flores T, Perez GM, Schmeidler J, Dickstein DL, Hof PR, Elder GA. Age-related vascular pathology in transgenic mice expressing presenilin 1-associated familial Alzheimer's disease mutations. Am J Pathol 2010;176:353–368.
34. Klein R, Knudtson MD, Klein BE, Zinman B, Gardiner R, Suissa S, Sinaiko AR, Donnelly SM, Goodyer P, Strand T, Mauer M. The relationship of retinal vessel diameter to changes in diabetic nephropathy structural variables in patients with type 1 diabetes. Diabetologia 2010;53:1638–1646.
35. Sorokin L. The impact of the extracellular matrix on inflammation. Nat Rev Immunol 2010;10:712–723.
36. Zhang AJ, Yu XJ, Wang M. The clinical manifestations and pathophysiology of cerebral small vessel disease. Neurosci Bull 2010; 26:257–264.
37. Engler A, Bacakova L, Newman C, Hategan A, Griffin M, Discher D. Substrate compliance versus ligand density in cell on gel responses. Biophys J 2004;86(1 Pt 1):617–628.
38. Barakat A, Lieu D. Differential responsiveness of vascular endothelial cells to different types of fluid mechanical shear stress. Cell Biochem Biophys 2003;38:323–343.
39. Barakat AI. Responsiveness of vascular endothelium to shear stress: Potential role of ion channels and cellular cytoskeleton (review).Int J Mol Med 1999;4:323–332.
40. Zhu Y, Liao HL, Niu XL, Yuan Y, Lin T, Verna L, Stemerman MB. Low density lipoprotein induces eNOS translocation to membrane caveolae: The role of RhoA activation and stress fiber formation. Biochim Biophys Acta 2003;1635:117–126.
41. Navarro A, Anand-Apte B, Parat MO. A role for caveolae in cell migration. Faseb J 2004;18:1801–1811.
42. Kabouridis PS, Janzen J, Magee AL, Ley SC. Cholesterol depletion disrupts lipid rafts and modulates the activity of multiple signaling pathways in T lymphocytes. Eur J Immunol 2000;30:954–963.
43. Raucher D, Sheetz MP. Cell spreading and lamellipodial extension rate is regulated by membrane tension. J Cell Biol 2000;148: 127–136.
44. Wakatsuki T, Wysolmerski RB, Elson EL. Mechanics of cell spreading: Role of myosin II. J Cell Sci 2003;116(Pt 8):1617–1625.